Indian Journal of Chemical Technology
Vol. 31, November 2024, pp. 860-867
DOI: 10.56042/ijct.v31i6.11597

Radiation absorption properties of some metals used as biomaterials

Aycan ŞENGÜL[1]*, Kadir AKGÜNGÖR[2], Kadir GÜNOĞLU[3] & Iskender AKKURT[4]

[1]Akdeniz University, Vocational School of Health Services, Medical Imaging Program, 07058, Antalya, Turkey

[2]Dokuz Eylul University, Faculty of Science, Department of Physics, Department of Atomic and Molecular Physics Izmir, Turkey

[3] Isparta Applied Science University, Vocational School of Technical Sciences, Nuclear Technology and Radiation Safety, Isparta, Turkey

[4]Suleyman Demirel University, Faculty of Engineering and Natural Sciences, Department of Physics, Isparta, Turkey

*E-mail: aycansahin@akdeniz.edu.tr

Received 3 June 2024; accepted 17 September 2024

The aim of the study is to evaluate some basic gamma-ray attenuation properties of various types of biomaterials used in the human body as synthetic or natural materials. GAMOS 6.2 is used to compute the Linear Attenuation Coefficient (LAC). Other critical parameters Half Value Layer (HVL), Tenth Value Layer TVL, and Mean Free Path (MPF) are determined as well. During the computational phase of the study, a mono-energetic point photon source geometry with energies ranging from 1 keV to 20 MeV is used by directing a parallel photon beam toward the absorber material using Monte Carlo software. Radiation shielding properties are measured in the experiment section of the study at 662, 1173, and 1332 keV. M3 has the best values for the investigated parameters. Furthermore, metal biomaterial M3 with Cr, Mn, Fe, Co, and Mo elements and 8.4 g/cm^3 density has the lowest HVL, TVL, and MPF values. According to our findings, M3 has exceptional gamma-ray attenuation properties in metal biomaterials. The Monte Carlo method is shown to be a viable option for calculating mass absorption coefficients at the desired gamma energy, especially for samples that are physically demanding to generate.

Keywords: Biomaterials, Gamma-ray attenuation, Metals, Monte Carlo, Linear attenuation coefficients

Introduction

Biomaterials are natural or synthetic materials utilized to interface with the biological environment or to heal, replace, or repair damaged or diseased tissue used in the human body. Medical devices that are implanted and extracorporeal are created using these materials. Investigators have discovered the necessity to improve biocompatibility since biomaterials are chosen based on mechanical, physical, and biological qualities. Medical and engineering experts have created biomaterials that interact with tissue for over 50 years. Biomaterials are used in various technologies today, including artificial hearts, pacemakers, artificial eyes, dental implants, and hip prostheses. Biomaterials utilized in the human body as either synthetic or natural substances serve a crucial tissue function[1-5].

Since its discovery, radiation has been put to numerous uses, including energy production in power plants, radiological applications in medicine, foundational scientific research, and industrial applications. By producing ionization and excitation interactions in the irradiated material medium, indirect ionizing radiation transports energy. These interactions vary depending on the incoming photon's energy and the absorbing medium's composition[6]. Gamma radiation can penetrate the human body, ionizing and destroying tissue[7, 8]. Consequently, gamma-ray shielding is of most significance to scientists, and numerous recent studies have been conducted in this area. The attenuation coefficient quantifies the likelihood of photon scattering or absorption interactions per unit mass of the absorbing medium. However, there are literature studies for μ/ρ based on experimental[9-30] or computational assessments [8, 16, 18, 30-50]. For a few materials, the possibility of photons entering scattering or absorption interactions per unit mass of the absorbing medium is represented by the attenuation coefficient (μ/ρ), which is estimated at specific energy points or by computer analysis.

This work aims to calculate μ/ρ data using the Monte Carlo method for various metals in the energy range 1 keV-20 MeV and to compare them with both experimental data and XCOM. This technique permits the determination of Linear Attenuation Coefficient (LAC) over a broad energy range for any element, compound, or mixture, based on a simple geometry

model, source identification, and elemental weight percentages of the compounds. In the simulations performed with GAMOS a single-energy point photon source geometry was used by directing a parallel photon beam onto an absorber material

Experimental Section

Gamma rays with energies of 662, 1173, and 1332 keV emitted by ^{137}Cs and ^{60}Co radioactive sources were used in the experiment, and attenuation coefficients were calculated. The measurements were made with a gamma spectrometer system that included NaI(Tl) and a 16k multichannel analyzer in The Physics Department of the Faculty of Science at Süleyman Demirel University [49]. The components above were attached to the A Maestro software application to convert the electric signal obtained from the multi-channel analyzer to a count. The detector was ringed with lead to reduce background radiation, as seen in Fig. 1. Background measurements were acquired separately and eliminated from the original spectra. This approach has been employed in several experimental research[50, 54].

The radioactive sources used in this experiment were ^{137}Cs and ^{60}Co. When gamma rays reach an absorber of a specific thickness, some photons are absorbed while others pass through. Use the following equation to determine the LAC (μ) for this process.

$$I = I_o e^{-\mu x} \quad \ldots(1)$$

I_o is the starting number of gamma-ray counts (recorded in the detector), I is the number of gamma-ray counts that pass through the glass, μ is the LAC of the shielding material in cm^{-1}, and x is the absorber thickness in cm. Fig. 2 shows an energy spectrum for the ^{137}Cs and ^{60}Co sources based on the number of counts collected in the detector. The difference between the quantity of gamma radiation captured with and without the absorber is striking.

The Monte Carlo technique is a statistical approach frequently utilized in research and engineering. The method employs pseudo-random numbers and probability distributions to determine the mean of a difficult-to-calculate analytically or numerically physical property. It is highly applicable to radiation transport problems with some knowledge of beam parameters and elemental composition [56].

This study calculates the LAC of specific biomaterials (such as metal) using the well-known Monte Carlo method. The simulations employ a photon source that emits monoenergetic photons in a parallel beam toward a cylindrical absorber with a NaI detector situated behind it. 36 distinct photon energies ranging from 1 keV to 20 MeV were utilized to perform the simulations.

The Monte Carlo software tool for simulating neutrons, gamma rays, and electron transport was employed in this study to simulate and then calculate the new materials' attenuation characteristics[51]. GAMOS (Geant4-based Architecture for Medicine-Oriented Simulations) is a fork of the well-known Monte Carlo software Geant4. It is used by medical physicists to model radiation sources in clinical settings[52]. GAMOS provides physics programs for coping with numerous particles over a broad range of energies and scoring programs for determining the necessary particle characteristics. Although GAMOS was initially developed for medical physics simulations, it has been designed to accommodate the widest spectrum of users possible by minimizing errors associated with fundamental C++ knowledge [51,52]. GAMOS now has over 2500 registered members globally and is quickly increasing[56].

The GAMOS 6.2 software was used to predict the element compositions, geometries, and radiation interaction characteristics of biomaterials in this investigation. The simulations in this work comprise a point photon source in a cylinder that generates mono-energetic photons directed parallel toward a cylindrical sample 20 cm distant from the source. The detector was designed as a NaI and was placed 50 cm distant from the source.

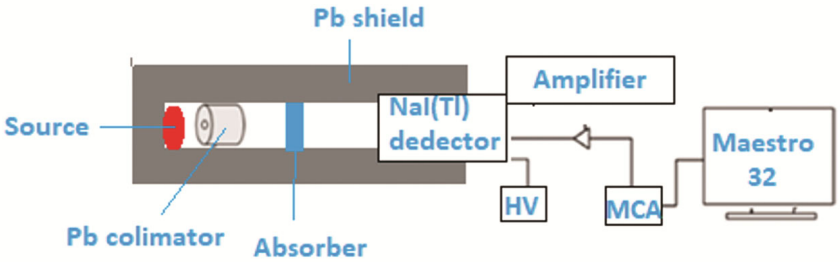

Fig. 1 — A diagram of NaI detector for experimental measurements

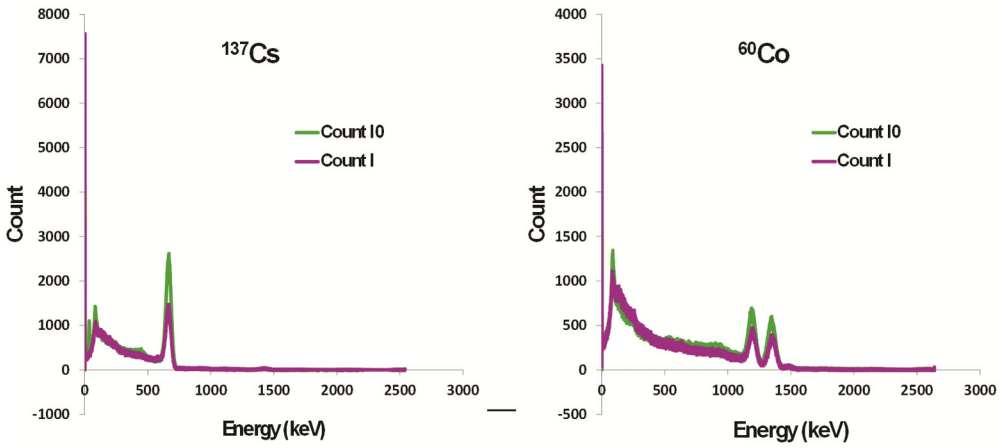

Fig. 2 — Spectra of attenuated and original -rays obtained from ^{137}Cs and ^{60}Co sources

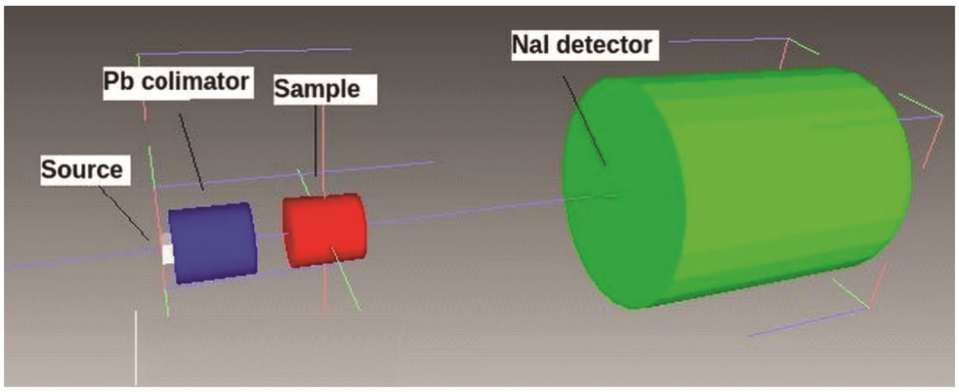

Fig. 3 — Utilization of the GAMOS model geometry for calculation μ/ρ

As depicted in Fig. 3, the entire simulation configuration corresponds to the narrow beam geometry constraints used in attenuation coefficient experiments, guaranteeing that there is no contribution from scattered photons[6].

The electromagnetic physics package is the physics package utilized in the simulation. All particles reaching the surface with the surface flow were tallied during scoring, and the spectrum was derived using a classifier. The simulation was run with and without absorbing material for each energy. While all physical processes were scored, no variance reduction strategies were applied. Each simulation took around 20 h to compute, and no parallel processing was employed. The number of 10^7 photons, which produces good results, is used to boost the precision of Monte Carlo computations and to generate minimal statistical error. The simulations were run on an Intel Xeon 3.9 GHz workstation with 64 GB of RAM.

Due to their superior mechanical qualities, metals, and their alloys, among the most popular materials in the biomaterials industry, are very significant. To avoid deterioration in the biological environment inside the body, metallic biomaterials should be corrosion-resistant and free of toxins and allergic reactions. The metallic biomaterial used in place of bone is anticipated to match the mechanical characteristics of bone [1, 2, 5, 60, 61].

Bone replacement material and joint prosthesis in orthopedic applications, defect repair material in facial and maxillofacial surgery, in trauma treatments, as a substructure in dentally removable and fixed prostheses, and subperiosteal and endosteal dental implants and cardiovascular surgery, application of artificial heart parts, catheter, heart valve [60,61]. Elemental analyses of materials employed in the research Table 1 is provided.

Results and Discussion

The I_o measurement was taken, also known as the reference measurement. Although there is no sample between the radioactive source and the detector, the

Table 1 — Properties of the metal materials examined in the study

Material	Density (g/cm^2)	Thickness (mm)	C	O	Al	Si	Ti	V	Cr	Mn	Fe	Co	Mo
M1	4.45	10	4.41		5.8		85.58	4.21					
M2	8.3	12	3.85		6.09		85.86	4.19					
M3	8.4	10	8.18	2.05		0.41			24.69	1.19	0.46	58.09	4.92

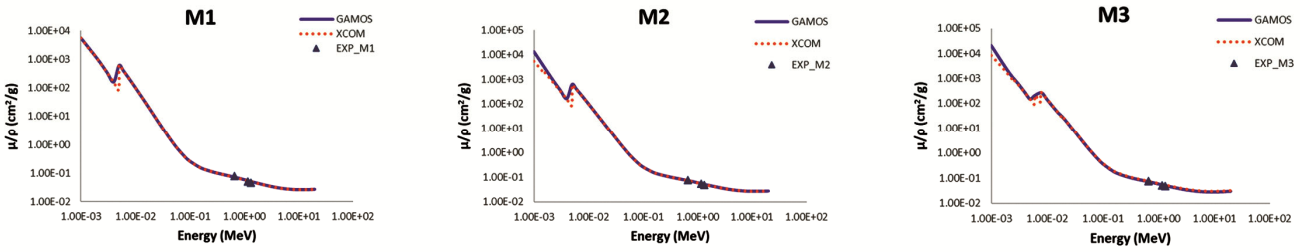

Fig. 4 — Comparison of measured, calculated and XCOM mass attenuation coefficients at different gamma energies for metals

intensity of the source's radiation was measured over time. This I_o reference measurement was used for all biomaterials. In the second stage, the material was positioned between the source and the detector, and I, representing the attenuated radiation intensity, was measured. The source-detector and source-sample distances for each source and the measurement times for all samples were the same in the experiments[14].

At gamma energies varying from 1 keV to 20 MeV, the mass attenuation coefficient (μ/ρ) values were retrieved using the XCOM algorithm. The XCOM results are shown in Fig. 4, where the modeling and experimental data are compared. When the results for the three metals are compared, there is explicit good agreement between experimental and computational data. Furthermore, for three materials, the highest values of μ/ρ are at lower energies, while the lowest values are at higher energies. The jumps seen in the graphs are due to the photoelectric effect around the K-edge of the material. These examples are materials containing elements with high atomic numbers (Ti, Cr, Mn, Fe, and Co). As seen in the comparison of M1, M2, and M3 samples in Fig. 5, the differences between the values in this region are much larger than in other areas.

The gamma-ray versus LAC plot for the GAMOS simulations is shown in Fig. 5. The graphs show that the LAC decreases as energy levels rise, and stable behaviour is achieved at higher energy levels. This implies that the LAC is significantly energy dependent at low energy levels but practically constant at high.

This tendency can be explained by two factors: first, at higher energies, all materials absorb nearly

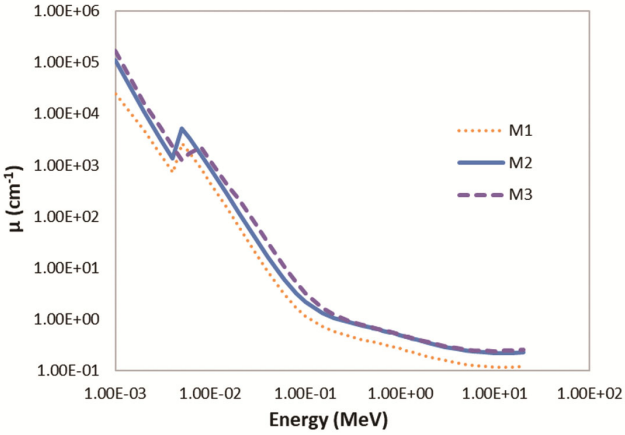

Fig. 5 — Comparison of measured and calculated LAC at different gamma energies for the metals

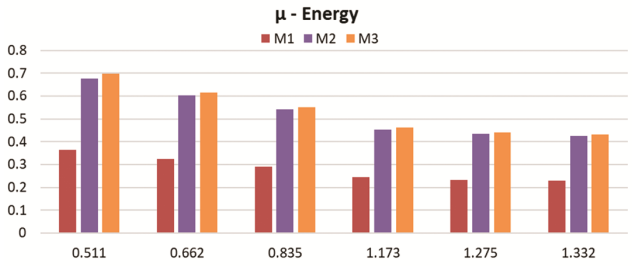

Fig. 6 — LAC of various gamma energies for the metals

the same amount of radiation, and second, in different energy ranges, distinct absorption mechanisms are prominent. Fig. 6 depicts the LAC values obtained from GAMOS simulations for the selected materials to aid comprehension of the results.

Using the computer program MAESTRO32, the spectral regions were calculated during the analysis of

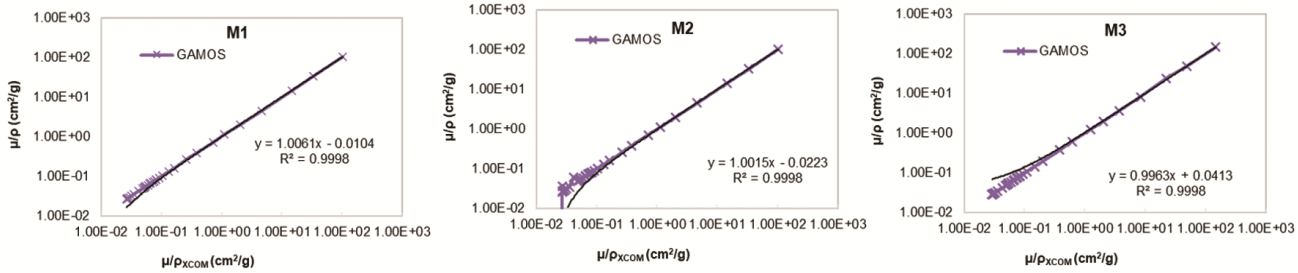

Fig. 7 — (μ /ρ) from Monte Carlo simulations plotted against data from the XCOM database

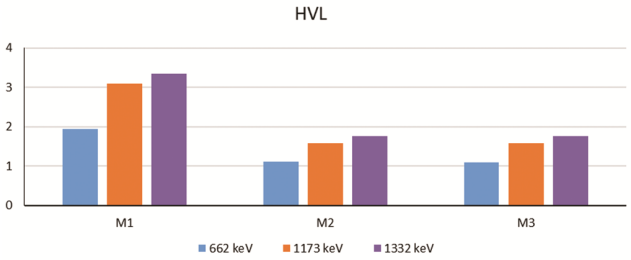

Fig. 8 — HVL values for metals

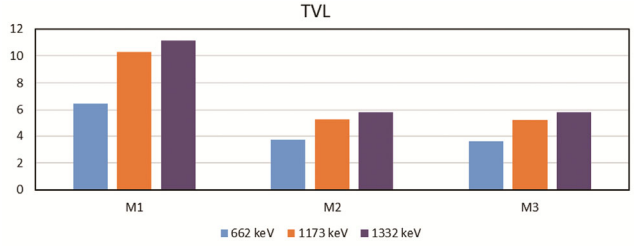

Fig. 9 — TVL values for metals

the spectra obtained as a consequence of the measurements[61]. Where x is the material thickness and I and I_0 are the background-subtracted counts recorded in the detector with and without material between the detector and the source, respectively, Eq. (1) describes the relationship between the material thickness and the background-subtracted counts.

$$I = I_o e^{-\mu x} \quad \ldots (1)$$

The XCOM program, developed by Berger and Hubbel, is a highly effective method for theoretical calculations free of elements, compounds, or mixtures at energies ranging from 1 keV to 100 GeV[62]. The mass attenuation coefficients at photon energies ranging from keV to GeV are calculated using a PC-based data bank that uses pre-existing data bases for coherent and incoherent scattering, photoelectric absorption, and pair formation cross-sections. The mass attenuation coefficients were calculated using the algorithm and the material's density. It was observed that the results of the GAMOS were found to produce consistent results when compared with the results of XCOM[62]. XCOM and GAMOS results show similar trends for M1, M2 and M3 materials, respectively, as shown in Fig. 7. (R^2>0.99).

The HVL concept is frequently used to evaluate the radiation attenuation effect of a material to be used as a gamma radiation shield (Fig. 8) [63-65]. This idea states that the shield material's thickness should equal half the intensity of the incoming radiation plus the intensity of the attenuated radiation in Eq. (2).

$$HVL = \frac{ln2}{\mu} \quad \ldots (2)$$

In the case of the TVL, it is defined as the thickness of material required to block 10% of the radiation in glasses and is calculated using Eq. 3.

$$TVL = \frac{ln10}{\mu} \quad \ldots (3)$$

The MFP parameter computes the average distance between two subsequent collisions. As the distance between two successive interactions MFP decreases, the number of contacts between entering photons and material atoms rises, and therefore absorption and attenuation increase [66,67]. MFP is comparable in that it can be derived from the LAC values, as given in Eq. (4).

$$MFP = \frac{1}{\mu} \quad \ldots (4)$$

For M1, M2, and M2 materials, we examined the variation of the reduction coefficient with density and the HVL (Fig. 8), TVL (Fig. 9), and MFP (Fig. 10) values. For all metals, it is seen in Fig. 10 that the LAC increase with increasing material density. Similar results were obtained for all energies. It has been shown in many studies in the literature that the LAC increase as the density increases.

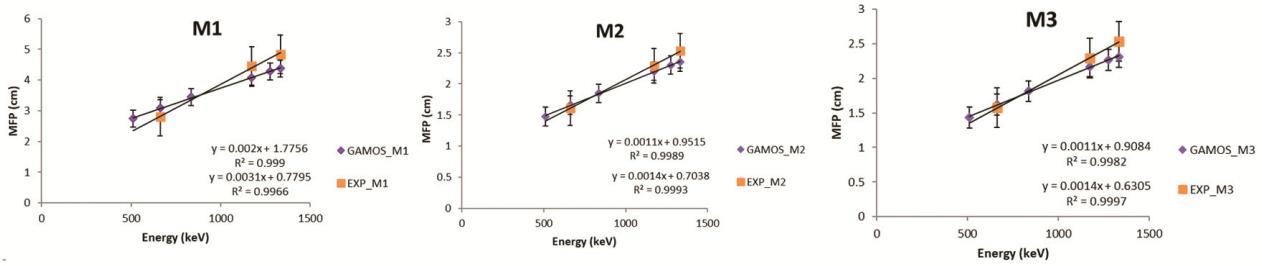

Fig. 10 — MFP as a function of energy

Conclusion

Monte Carlo computations were conducted at various gamma energies to assess the radiation shielding efficacy of multiple metal materials applied within the human body, both natural and manufactured. The findings of the mass absorption coefficients initially show a considerable decline in the energy range where photoelectric absorption predominates depending on the material's atomic number. Following this initial increase, all biomaterials demonstrate a steady decrease with a virtually identical trajectory, with the atomic number dependency vanishing in μ/ρ values. This final trend is explained by the increased dominance of Compton scattering at medium and high energy. With increasing gamma energy, HVL and TVL grow. Results from the experiment and the GAMOS data were comparable. MFP data make it quantities evident that a gamma with low energy loses energy quickly whereas a gamma with more energy can travel farther. An excellent agreement (R^2 = 0.99) was found when the obtained values were compared to both the theoretical values of the XCOM database and the experimental results. The acceptable variations between test and simulation results can be attributed to uncertainties caused by poor geometry conditions in the experimental setup. M3 has the best values for the investigated parameters. Furthermore, metal biomaterial M3 with Cr, Mn, Fe, Co, and Mo elements and 8.4 g/cm^3 density had the lowest HVL, TVL, and MPF values. According to our findings, M3 has exceptional gamma-ray attenuation properties in metal biomaterials. These findings demonstrate that the Monte Carlo approach can be used safely even in the presence of constraints like the constrained gamma energies used in a laboratory setting or the incapacity to conduct measurements due to the difficulties in physically producing the material.

References

1 Parida P, Behera A & Mishra S C, *Classification of Biomaterials used in Medicine, Int J Adv Appl Sci,* 1 (2012) 125.

2 Park J & Lakes R S, *Biomaterials: an introduction*. 2007: Springer Science & Business Media.

3 Benson R S, Nuclear instruments and methods in physics research section B: Beam interactions with materials and atoms, *Use of Radiation in Biomaterials Science*, 191 (2002) 752.

4 Chen F M & Liu X, Advancing biomaterials of human origin for tissue engineering, *Progress Polym Sci*, 53 (2016) 86.

5 Yazdi M K, Zare M, Khodadadi A, Seidi F, Sajadi S M, Zarrintaj P, Arefi A, Saeb M R & Mozafari M, Polydopamine biomaterials for skin regeneration, *ACS Biomater Sci Eng*, 8 (2022) 2196.

6 Johnson T E, *Introduction to Health Physics, 5th Edn,* McGraw-Hill Education, (2017).

7 Mahmoud K, Sayyed M & Tashlykov O, Gamma ray shielding characteristics and exposure buildup factor for some natural rocks using MCNP-5 code, *Nucl Eng Technol*, 51 (2019) 1835.

8 Akkurt I, Akyıldırım H, Mavi B, Kilincarslan S & Basyigit C, Photon attenuation coefficients of concrete includes barite in different rate, *Ann Nucl Energy*, 37 (2010) 910.

9 Al-Buriahi M S, Arslan H & Tonguç B T, Mass attenuation coefficients, water and tissue equivalence properties of some tissues by Geant4, XCOM and experimental data, *Indian J Pure Appl Phys*, 57 (2019) 433.

10 Phelps M E, Hoffman E J & Ter-Pogossian M M, Attenuation coefficients of various body tissues, fluids, and lesions at photon energies of 18 to 136 keV, *Radiology*, 117 (1975) 573.

11 Sahin A & Bozkurt A, Monte Carlo Calculation of Mass Attenuation Coefficients of Some Biological Compounds, *Süleyman Demirel Üniversitesi Fen Edebiyat Fakültesi Fen Dergisi*, 14 (2019) 408.

12 Patterson D K, Pepperberg I M, Story B H & Hoffman E A, How parrots talk: Insights based on CT scans, image processing and mathematical models, Physiology and Function from Multidimensional Images - Medical Imaging 1997, Eds Hoffman E A, Bellingham, *Spie Int Soc Optical Eng*, 3033 (1997) 14.

13 Akkurt I, Malidarre R B & Kavas T, Monte carlo simulation of radiation shielding properties of the glass system containing Bi_2O_3, *Eur Phys J Plus*, 136 (2021) 1.

14 Akkurt I, Calik A & Akyıldırım H, The boronizing effect on the radiation shielding and magnetization properties of AISI 316L austenitic stainless steel, *Nucl Eng Design*, 241 (2011) 55.

15 Cena B, Determination of the type of radioactive nuclei and gamma spectrometry analysis for radioactive sources, *Int J Comput Exp Sci Eng*, 10 (2024) 321

16 Karpuz N, Effective atomic numbers of glass samples, *Int J Comput Exp Sci Eng*, 10 (2024) 340.

17 Akkurt I, Malidarre R B, Kartal I & Gunoglu K, Monte carlo simulations study on gamma ray–neutron shielding characteristics for vinyl ester composites, *Polym Compos*, 42 (2021) 4764.

18 Almisned G, Akkurt I, Tekin H O, Dicle I Y & Doğan S Ö, Gamma ray shielding properties of CeO_2-added hydroxyapatite composite, *J Aust Ceram Soc*, 58 (2022) 1.

19 Kutu N, Neutron shielding properties of cellulose acetate CdO-ZnO polymer composites, *Int J Comput Exp Sci Eng*, 10 (2024) 322.

20 Sayyed M, Kaky K M, Gaikwad D K, Agar O, Gawai U P & Baki S O, Physical, structural, optical and gamma radiation shielding properties of borate glasses containing heavy metals (Bi_2O_3/M_oO_3), *J Non-Cryst Solids*, 507 (2019) 30.

21 Mears D, Metals in medicine and surgery, *Int Metals Rev*, 22 (1977) 119.

22 Dong Q & Fang Y, Metal-halide perovskites for high-efficiency radiation shielding applications, *Light Sci Appl*, 12 (2023) 8.

23 Syla N, Ahmeti H, Aliaj F & Dalipi B, The determination of some sizes and physical characteristics of metals by ultrasound, *Int J Comput Exp Sci Eng*, 10 (2024) 315.

24 Celen Y Y, Gunay O, Oncul S & Narin B, Measurement of soil radon concentration in Balikesir and examination of its effects on health, *J Radiat Res Appl Sci*, 16 (2023) 100718.

25 Oruncak B, Radiation shielding properties for 90(Se)- (10-x) (Te)-x(Ag) chalcogenide glasses, *J Radiat Res Appl Sci*, 16 (2023) 100723.

26 Karpuz N, Radiation shielding properties of glass composition, *J Radiat Res Appl Sci*, 16 (2023) 100689.

27 Akkurt I & El-Khayatt A, Effective atomic number and electron density of marble concrete, *J Radioanal Nucl Chem*, 295 (2013) 633.

28 Bozkurt A & Sengul A, Monte carlo approach for calculation of mass energy absorption coefficients of some amino acids, *Nucl Eng Technol*, 53 (2021) 3044.

29 Ermis E, Pilicer F B, Pilicer E & Celiktas C, A comprehensive study for mass attenuation coefficients of different parts of the human body through monte carlo methods, *Nucl Sci Techniques*, 27 (2016) 54.

30 Akkurt I & Akyıldırım H, Radiation transmission of concrete including pumice for 662, 1173 and 1332 keV gamma rays, *Nucl Eng Des*, 252 (2012) 163.

31 Akkurt İ, Gunoglu K, Basyigit C & Akkas Ayşe, Hafif betonların 511 ve 1275 keV'deki radyasyon zayıflatma katsayılarının araştırılması, *Süleyman Demirel Üniversitesi Fen Bilimleri Enstitüsü Dergisi*, 16 (2012) 315.

32 Jawad A, Demirkol N, Gunoğlu K & Akkurt I, Radiation shielding properties of some ceramic wasted samples, *Int J Environ Sci Technol*, 16 (2019) 5039.

33 Gunoglu K & Akkurt İ, Radiation shielding properties of concrete containing magnetite, *Prog Nucl Energy*, 137 (2021) 103776.

34 Şengül A A K & Akkurt I, Gamma-ray shielding properties of some dosimetric materials, *J Aust Ceram Soc*, 59 (2022) 1.

35 Kassab L, Issa S A M, Mattos G R, Almisned G, Bordon C D S & Tekin H O, Gallium (III) oxide reinforced novel heavy metal oxide (HMO) glasses: A focusing study on synthesis, optical and gamma-ray shielding properties, *Ceram Int*, 48 (2022) 14261.

36 Bakıcıerle G, Şişman G & Akgüngör K, Estimating the dose differences nearby the metal implant by means of artificial contouring errors via Monaco and Geant4, *Revista Mexicana de Física*, 68 (2022) e51101.

37 Şengül A, Gamma-ray attenuation properties of polymer biomaterials: Experiment, XCOM and GAMOS results, *J Radiat Res Appl Sci*, 16 (2023) 100702.

38 Sengul A, Karpuz N, Akkurt I, Atik I, Malidarre R B, Sayyed M I & Arslankayaet S, Computation of the impact of NiO on physical and mechanical properties for lithium nickel phosphate glasses, *J Radiat Res Appl Sci*, 16 (2023) 100737.

39 Almuqrin A H, Sayyed M I, Kumar A, El-bashir B O & Akkurt I, Optical, mechanical properties and gamma ray shielding behavior of TeO_2-Bi_2O_3-PbO-MgO-B_2O_3 glasses using FLUKA simulation code, *Opt Mater*, 113 (2021) 110900.

40 Boodaghi-Malidarre R, Akkurt I & Kavas T, Monte carlo simulation on shielding properties of neutron-gamma from 252Cf source for Alumino-Boro-Silicate glasses, *Radiat Phys Chem*, 186 (2021) 109540.

41 Akkurt I & Malidarre R B, Physical, structural, and mechanical properties of the concrete by FLUKA code and phy-X/PSD software, *Radiat Phys Chem*, 193 (2022) 109958.

42 Kartal İ & Selimoğlu H, Usability of pine sawdust and cotton together as filler in recycled polypropylene composites, *Int J Comput Exp Sci Eng*, 10 (2024) 244.

43 Coskun A, Cetin B, Yigitoglu I & Topakli H, Comparison of the radiation absorption properties of PbO doped ZrB_2 glasses by using GATE-GEANT4 monte carlo code and XCOM program, *Int J Comput Exp Sci Eng*, 9 (2023) 274.

44 Aygun Z & Aygun M, An analysis on radiation protection abilities of different colored obsidians, *Int J Comput Exp Sci Eng*, 9 (2023) 170.

45 Rwashdi Q A A D, Faez W, Gunoglu K & Akkurt İ, Experimental testing of the radiation shielding properties for steel, *Int J Comput Exp Sci Eng*, 8 (2022) 74.

46 Akkurt İ, Waheed F, Akyildirim H & Gunoglu K, Performance of NaI (Tl) detector for gamma-ray spectroscopy, *Indian J Phys*, 96 (2021) 1.

47 Akkurt I, Effective atomic and electron numbers of some steels at different energies, *Ann Nucl Energy*, 36 (2009) 1702.

48 Akkurt İ, Waheed F, Akyildirim H & Gunoglu K, Monte carlo simulation of a NaI(Tl) detector efficiency, *Radiat Phys Chem*, 176 (2020) 109081.

49 Andreo P, Monte carlo techniques in medical radiation physics, *Phys Med Biol*, 36 (1991) 861.

50 Glaser A K, Kanick S C, Zhang R, Arce P & Pogue B W, A GAMOS plug-in for GEANT4 based monte carlo simulation of radiation-induced light transport in biological media, *Biomed Opt Exp*, 4 (2013) 741.

51 Arce P, Mendes P R, Canadas M & Lagares J I, *GAMOS: A Geant4-based easy and flexible framework for nuclear medicine applications*, *IEEE Nuclear Science Symposium Conference Record*, 2008.

52 Arce P, Lagares J I, Harkness L, Pérez-Astudillo D, Cañadas M, Rato P, María de P, Abreu Y, Gianluca de L, Kolstein M & Díaz A, Gamos: A framework to do Geant4 simulations in different physics fields with an user-friendly interface, *Nuclear Instruments and Methods in Physics Research Section A: Accelerators, Spectrometers, Detectors and Associated Equipment,* 735 (2014) 304.

53 Collaboration G & Agostinelli S, GEANT4–a simulation toolkit, *Nucl Instrum Meth A*, 506 (2003) 250.

54 (a) Agostinelli S *et al*., GEANT4—A Simulation Toolkit, *Nuclear Instrumentation and Methods in Physics Research Section A*, 506 (2003) 250; (b) J. Allison*, et al.*, Geant4 developments and applications, *IEEE Transactions on Nuclear Science*, 53 (2006) 270.

55 Osman V G, Aycan S & Hikmettin D Effects of radiation at different dose rates on hematologic parameters in rats, *J Radiat Res Appl Sci*, 17 (2024) 100873.

56 Osman V G, Buyukcizmeci N & Basaran H, Dosimetric evaluation of three-phase adaptive radiation therapy in head and neck cancer, *Radiat Phys Chem*, 202 (2023) 110588.

57 Meral, M., *Çok İşlevli Uyluk Çivisi Tasarımı, Üretimi Ve Mekanik Özellikleri*. 2013, Fen Bilimleri Enstitüsü.

58 Osman V G & Mursel D, Effect of different CTV shrinkage and skin flash margins on skin dose for left chest wall IMRT: A dosimetric study, *Radiat Phys Chem*, 216 (2024) 111445.

59 Osman V G, Experimental evaluation of out-of-field dose for different high-energy electron beams and applicators used in external beam radiotherapy, *Radiat Phys Chem*, 215 (2024) 111345.

60 Wang L, Lai R, Zhang L, Zeng M & Fu L, Emerging liquid metal biomaterials: From design to application, *Adv Mater*, 34 (2022) 2201956.

61 Gao W, Wang Y, Wang Q, Ma G & Liu J, Liquid metal biomaterials for biomedical imaging, *J Mater Chem B*, 10 (2022) 829.

62 MAESTRO, *MAESTRO Software User's Manual*, (2021).

63 Berger M, Hubbell J H, Seltzer S M, Chang J, Coursey J S, Sukumar R, Zucker D S & Olsen K, XCOM: Photon cross sections database, *NIST PML Radiat Phys Div*, (2019).

64 Akman F, Kaçal M R, Sayyed M I & Karataşet H A, Study of gamma radiation attenuation properties of some selected ternary alloys, *J Alloys Comp*, 782 (2019) 315.

65 Al-Hadeethi Y & Sayyed M I, Gamma radiation attenuation characteristics for lithium-zinc-tellurite glasses using Geant4 code and PDS computer software, *Ceram Int*, 47 (2021) 1660.

66 Yazici S D, Günay O, Tunçman D, Kesmezacar F F, Yeyİn N, Aksoy S H & Çavdar K S, Evaluating radiation exposure to oral tissues in C-arm fluoroscopy a dose analysis, *Int J Comput Exp Sci Eng*, 10 (2024) 313.

67 Kutu N, Gamma ray shielding properties of the $57.6TeO_2$-38.4ZnO-4NiO system, *Int J Comput Exp Sci Eng*, 10 (2024) 310.

68 Şen B D, A novel approach for Technetium-99m radioisotope transportation and storage in lead-free glass containers: A comprehensive assessment through monte carlo simulation technique, *Int J Comput Exp Sci Eng*, 10 (2024) 304.